Nuclear Physics A541 (1992) 433–442
North-Holland

NUCLEAR
PHYSICS A

Positive-pion absorption on carbon at low pion energies

Yu.K. Akimov[a], M.G. Gornov[b], M.I. Gostkin[a], Yu.B. Gurov[b], I.I. Haysak[a], S.P. Kruglov[c], S.I. Merzlyakov[a], K.O. Oganesyan[a], E.A. Pasyuk[a], S.Yu. Porokhovoy[a], A.I. Rudenko[a], A.V. Shishkov[b] and I.I. Strakovsky[c]

[a] *Joint Institute for Nuclear Research, Head Post Office, Box 79, Moscow 101000, Russia*
[b] *Moscow Physical Engineering Institute, Moscow, 115409, Russia*
[c] *Petersburg Nuclear Physics Institute, Gatchina, St. Petersburg 188350, Russia*

Received 18 October 1990
(Corrected 10 December 1991)

Abstract: The total cross section of positive-pion absorption on carbon with a two-proton final state at pion energies of 26–39 MeV has been measured. At a pion energy of 28.5 MeV some narrow structure exists in the energy dependence of the cross section.

E NUCLEAR REACTIONS: $^{12}C(\pi^+, pp)X$; $E = 26$–39 MeV; measured pion absorption $\sigma(E)$ versus particle energy.

1. Introduction

In spite of a few decades of experimental study of pion absorption on nuclei, there are many open questions in understanding this reaction. The study of this process is interesting not only for its own sake, but also its elucidation might give information on nonnucleonic degrees of freedom in nuclei, in particular multiquark states. A detailed review of the modern understanding of pion absorption on nuclei has recently been published [1]). A detailed discussion of the simplest reaction, $\pi^+ d \to pp$, is contained in a recent review [2]).

Intensive investigations have been focused on the reaction $\pi^+ d \to pp$, which is the dominating process of the pion absorption at intermediate energies. Detailed information exists at energies close to the Δ-isobar region ($T_\pi = 100$–250 MeV), but there are few data below 100 MeV. Fig. 1 shows the complete data set of the total cross section in the channel $\pi^+ d \to pp$. There are systematic inconsistencies between different data sets. It is important to point out that there are several low data points, which gave the impression of a sharp dip in the total cross section at a pion energy of $T_\pi = 28$ MeV ($\sqrt{s} = 2.041$ GeV).

Correspondence to: Dr. I.I. Strakovsky, Petersburg Nuclear Physics Institute, Gatchina, St. Petersburg 188350, Russia.

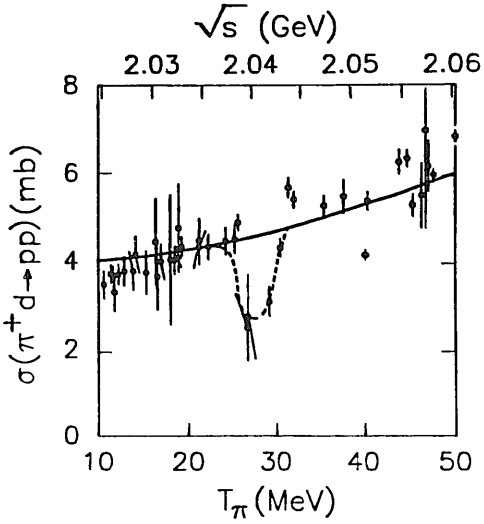

Fig. 1. Total cross section for the $\pi^+ d \to pp$ reaction. Data are from references contained in ref. [5]). Best-fit parameterization from ref. [6]) is shown by the solid curve.

There are only few papers containing experimental information concerning pion absorption on nuclei heavier than the deuteron at $T_\pi \leq 60$ MeV. Some of them [3]) reported the total absorption cross section without selection of any particular channel. In ref. [4]) the experimental data for the pion absorption with emission of two protons and a fixed state of the residual nuclei are presented. These data would be very important in the study of nuclear structure. Even if the formation of exotic states were sufficiently rare that their effect on the elastic-scattering cross section or the total reaction cross section would be negligible, one might still see their strong effect on individual partial cross sections. Low energies allow the pion to probe the nuclear volume, in contrast to the higher pion energy region that is sensitive to the surface of the nuclei only.

Here the first result of an investigation of pion absorption on carbon is presented. The reaction $^{12}C(\pi^+, pp)X$ with the detection of two protons in the final state at the pion kinetic energies of 26, 28, 30, 32, 36 and 39 MeV has been studied. Some possible interpretations are presented.

2. Experimental procedure

The measurements were carried out at the low-energy pion channel of the Petersburg Nuclear Physics Institute proton synchrocyclotron using a beryllium meson production target. The pion channel has a length of 8 m. Secondary particles are accepted at 60° with respect to the incident proton beam. A short pion channel is a very important feature, especially at low pion energies. The channel has two dipole magnets and seven quadrupole lenses and is arranged to provide a low level of muon contamination. To suppress the positron admixture the meson production target is oriented to present a minimum thickness with respect to the pion channel

direction. For the beam-content measurements, a time-of-flight system with timing relative to the radiofrequency of the accelerator was used. Fig. 2 shows the time-of-flight spectrum of the beam at a pion momentum of 114 MeV/c ($T_\pi = 39$ MeV). This spectrum was fitted by three gaussians, corresponding to pions, muons and positrons. The procedure provides an accuracy in the determination of the pion fraction in the beam to better than 1.5%. For the pion energy range 26–39 MeV the pion fraction smoothly varied from 63 to 78%. The muon contamination is approximately constant at the discussed energy region. The value of this contamination was 14% for the lowest energy and 12% for the highest one. The pion fraction decreases mainly due to the rise of positron fraction but not the muon one. Another part of the muon contamination is associated with pion decay at the last section of the channel and could not be resolved by the time-of-flight measurements. Monte Carlo simulation shows that its fraction in the beam slightly depends on the beam momentum and does not exceed 1% [ref. [7])] for this pion channel. The beam contents were monitored continuously during the measurements.

A thin semiconductor of 0.7 mm thickness placed inside the beam pipe was used for beam momentum centroid and width determination. The method is based on the fact that the channel accepts heavier charged particles such as p, d, t, etc., which have the same momentum but a sufficiently low energy and therefore short range that they stop in the semiconductor detector. In fact, the accuracy in the mean energy of the pion beam was better than 0.2 MeV. The energy losses of pions in the counters, foils and the target were taken into account to fit the beam energy in the

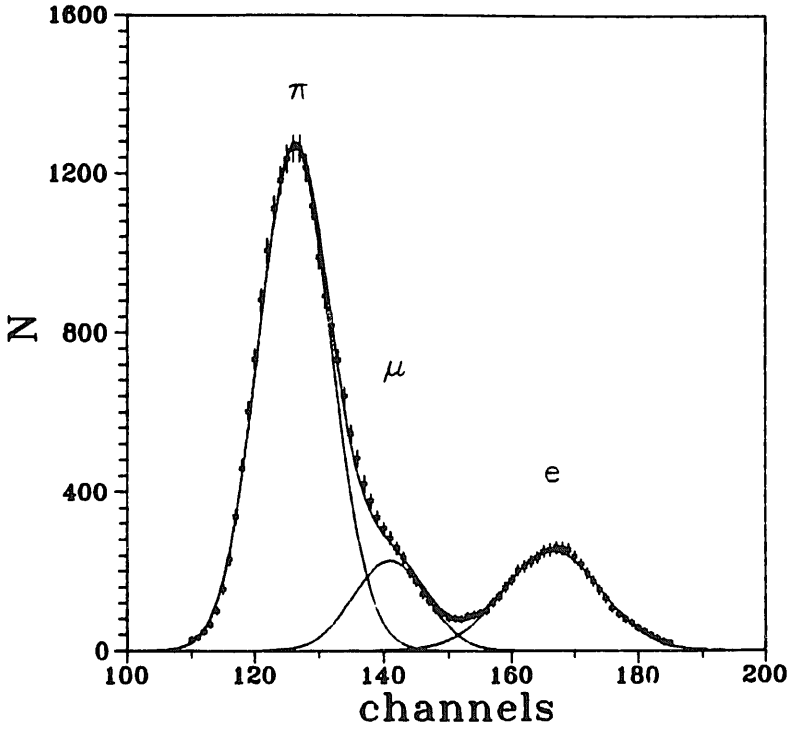

Fig. 2. Time-of-flight spectrum of the beam at pion momentum of 114 MeV/c. Solid line is the best fit.

center of the target. This procedure was repeated before and after each run. During a run the detector was removed from the beam.

The experimental setup is shown in fig. 3. It consists of the beam counters C1, C2 and veto counters C3, C4. C3 has a square hole of 3×3 cm^2. Counters C1 and C2 are used as a beam content and flux monitor and combined with C3 and C4 to trigger the scintillation hodoscope-spectrometer.

The momentum spread of the beam depends on the slit width of the copper collimator placed in the intermediate focus of the pion channel. For these measurements the energy spread was about 3 MeV (FWHM). The pion rate ($C1\times C2\times\overline{C3}$) was 10^3-10^4 s^{-1}. The beam was 4 cm in diameter (FWHM) at the inlet of the installation

The scintillation hodoscope-spectrometer [8]) has twelve plastic scintillation detectors, C5-C16, that are placed within the stainless-steel tank. This tank can be filled with a gas or vacuum-pumped when it is used for solid target and background measurements. The thickness of the scintillators is 10 cm, which is sufficient to stop outgoing particles originating from the pion absorption. These detectors are assembled in rectangular array. Four detectors are joined in a ring surrounding the beam. There are three such identical groups located sequentially along the beam axis. The rectangular "box" formed by the scintillators' surfaces has dimensions of $10\times10\times60$ cm^3. The longest axis of this "box" is oriented along the beam axis. When the inner volume is filled with a gas, it can be used as a target. If the solid target was used this volume was vacuum-pumped. Gaseous (H_2 and D_2) and solid (C) targets were used. This hodoscope covers the 4π solid angle almost completely and allows the measurement of the energies of outgoing particles with a resolution of approximately 10% for proton energies up to 100 MeV.

The spectrometer was calibrated using pp elastic scattering. For this measurement the tank was filled with gaseous hydrogen and the pion channel was tuned to obtain a proton beam with an energy about 60 MeV.

In the nuclear pion-absorption experiment a carbon target of 0.42 g/cm^2 thickness was used. It was placed in the center of the vacuum-pumped tank. Background measurements were carried out without target. The coincidence of signals from any two opposite walls of the hodoscope in coincidence with the signals from inbeam

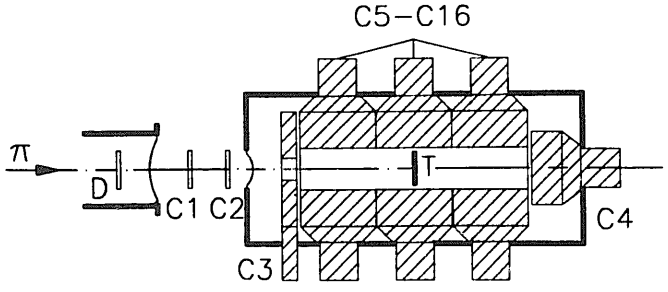

Fig. 3. Experimental setup.

counters C1, C2 and absence of signals from C3, C4 was used as trigger. Every event recorded on tape contains information about the energy deposition in each detector, time-of-flight and beam rate.

3. Data analysis

Final-state events with particles striking two opposite walls of the hodoscope and energies of each particle greater than 25 MeV were selected. Data for the central ring of the hodoscope corresponding to a 40°-140° angular interval for outgoing particles and opening angle greater than 90° were analyzed. Fig. 4 contains an example of the experimental two-particle energy spectrum obtained at a pion energy of 39 MeV with background subtracted. The measurements without target show that the background did not exceed 5% for the total event energies (T_{pp}) greater than 50 MeV and 1% above 110 MeV.

All the two-particle energy spectra show strongly pronounced maxima. Evidently, the high energy part of the spectra corresponds to the quasideuteron mechanism of the absorption. To extract these events, the high energy part of the spectrum was fitted excluding data below 110 MeV with a gaussian function. The solid line on fig. 4 shows the result of this fit.

Some tests were applied to the data to verify the validity of the procedure of quasideuteron event extraction. The peak position of the two-particle energy spectrum has a linear incident pion energy dependence with a slope equal to 0.99 ± 0.09 (fig. 5). This fact shows that the incident pion kinetic energy is distributed between

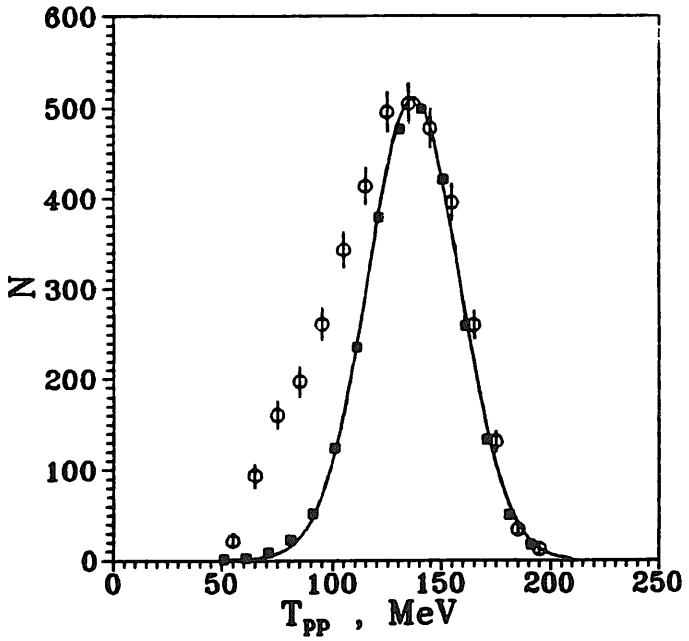

Fig. 4. Two-proton energy spectrum for the reaction $^{12}C(\pi^+, pp)X$ at pion energy of 39 MeV. Circles show experimental data, squares Monte Carlo simulation of the reaction $^{12}C(\pi^+, pp)^{10}B$; the solid line represents the best fit.

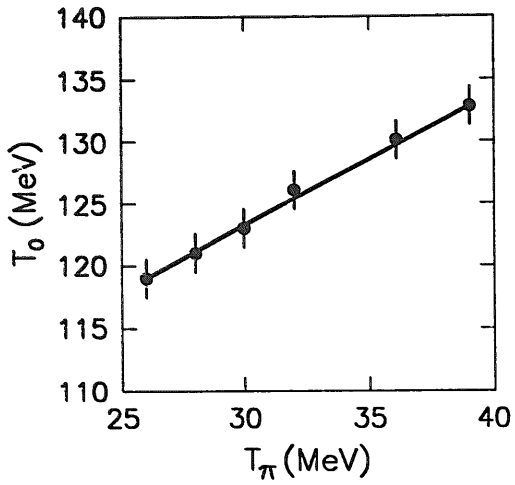

Fig. 5. Peak position of the two-proton energy spectrum versus pion kinetic energy. Solid line is the best fit.

the two final-state protons only. As additional test, the reaction $\pi^+ d \to pp$ was measured at the same conditions. Here the tank was filled by gaseous deuterium as a target. Fig. 6 shows the spectrum of two protons from the reaction $\pi^+ d \to pp$. The shift in the spectrum peak position (figs. 4 and 6) is due to different kinematics of the pion absorption on deuteron and carbon and the energy losses in the different targets. A Monte Carlo simulation of the process $^{12}C(\pi^+, pp)^{10}B$ has been done using the code FOWL [9]). The Monte Carlo simulation was performed according to a pure phase space, did not assume any dynamics and assumed that the residual

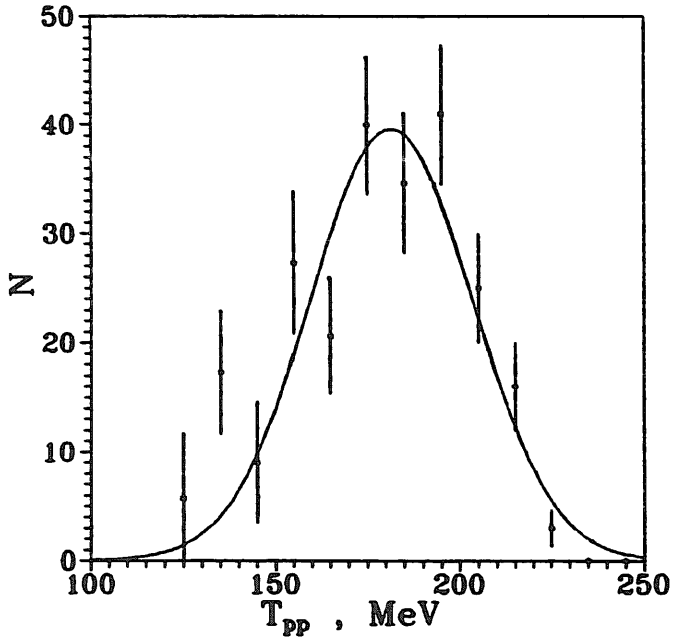

Fig. 6. Two-proton energy spectrum for the reaction $\pi^+ d \to pp$ at a pion energy of 39 MeV. Solid line is the best fit.

nucleus is in the ground state. The reaction was simulated with the actual geometry of this setup, taking into account energy losses in the carbon target. The results of this simulation are shown as squares in fig. 4. They are in a good agreement with the results of the best-fit procedure described above. The results of these tests prove the adequacy of the applied procedure of extraction of the quasideuteron absorption events. The rest of the events after extraction of the quasideuteron events is connected to other channels of absorption, for example neutron production, which is not detected by the spectrometer.

The value of the total cross section for the quasideuteron channel of the absorption was estimated using the total number of detected two-proton events and taking into account the experimental acceptance and geometry efficiency of the set-up. A Monte Carlo simulation was used to obtain the information about the acceptance and geometry efficiency of the set-up. The estimate shows 21 ± 4 mb of the cross section in the quasideuteron channel at $T_\pi = 39$ MeV. Because the real angular distribution on which the geometry efficiency depends is unknown, a large fraction (about 20%) of the absolute normalization uncertainty was assigned to the total cross section. It is well known that the angular distribution of protons from the reaction $\pi^+ d \to pp$ at low pion energies 25–40 MeV varies very slightly [5]). As the result, the relative uncertainties are ten times less.

It is interesting to point out that the ratio of the total cross sections for pion absorption on carbon and on deuteron is approximately equal to the atomic numbers ratio.

Fig. 7 shows the cross sections for the reaction $^{12}C(\pi^+, pp)X$ with the detection of two protons in the final state at the laboratory angular interval 40°–140°. Fig. 8 shows the same value for the quasideuteron events only.

The energy dependence of the quasideuteron process is approximately linear and its slope is close to that of the total cross section for the reaction $\pi^+ d \to pp$ [ref. [6])]. But, there is some narrow structure with a depth of roughly 12% nearby the pion

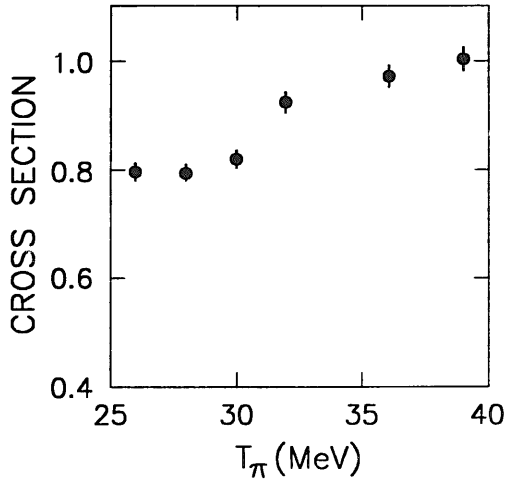

Fig. 7. Cross section versus pion kinetic energy for all events with $T_{pp} \geq 50$ MeV (in arbitrary units).

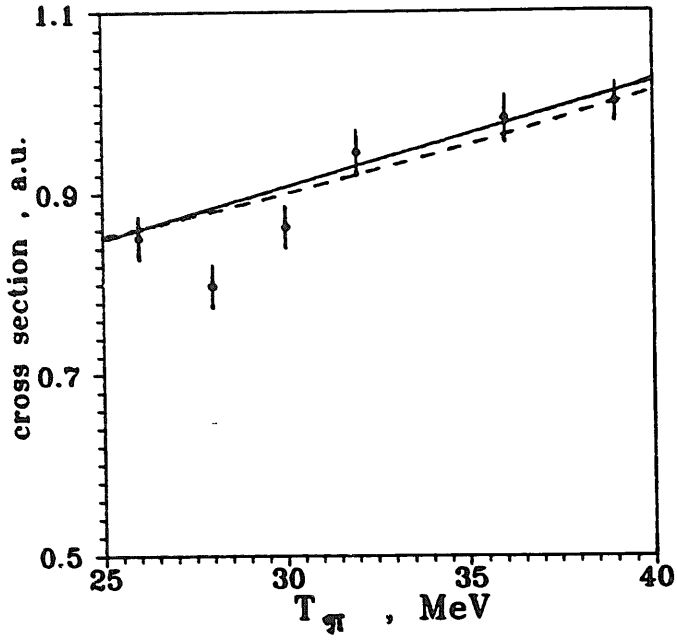

Fig. 8. Cross section versus pion kinetic energy for quasideuteron events (in arbitrary units). Solid line is the linear fit to experimental data excluding data at 28 and 30 MeV. Dashed line is the parameterization of the cross section for the reaction $\pi^+ d \to pp$ from ref. [6]) renormalized to the cross section at 39 MeV.

energy of 28.5 MeV. Since the energy spread of the beam was about 3 MeV, the intrinsic width of the structure is less then 3 MeV. The best-fit parametrization by a linear function of energy is shown by the solid curve in fig. 8. Using only data at $T_\pi = 26$, 32, 36 and 39 MeV, the χ^2 for a linear fit is equal to 0.95. For the complete set of data, including data at $T_\pi = 28$ and 30 MeV, χ^2 is equal to 13.8. Root mean-square deviation from linear energy dependence at both energies is equal to $(4\text{–}5)\sigma$.

4. Discussion

Some possible alternative nonconventional interpretations of the observed structure near 28.5 MeV include the following:

(i) A diproton in the nonstrange sector with isospin $T = 1$. In fact, fig. 1 shows the effect that might be caused by the interference of the resonant part of the dominant partial amplitude with the small angular momentum in the energy range under discussion and the imaginary part of the nonresonant contribution. Since the reaction $\pi^+ d \to pp$ is an inelastic process the interference here could be destructive. In fact, the differential cross section of the reaction $\pi^+ d \to pp$ [ref. [10])] proves the absence of partial waves with the large angular momentum $l \geq 3$ at this energy range.

The effect shown in fig. 1 is supported by the energy dependence of the total cross section of the pp triplet state with projection of spin equal zero with respect to the beam axis

$$\sigma_{T0} = \sigma^{\text{tot}} + \tfrac{1}{2}\Delta\sigma_{\text{L}} - \Delta\sigma_{\text{T}}$$

(fig. 9). The matrix element analysis

$$\sigma_{T0} \simeq \sum_J J \text{ Im } R_{J-1,J} + (J+1) \text{ Im } R_{J+1,J} - 2\sqrt{J(J+1)} \text{ Im } R^J$$

shows that σ_{T0} contains odd partial waves with orbital angular momentum not equal to total angular momentum (notation as was proposed in ref. [12]). There is no $^3P_0$ final state in the reaction $\pi^+ d \to pp$ due to parity conservation. As the result, the considered effects (figs. 1 and 9) could be caused by the diproton resonance in the $^3P_2$ NN state. Certainly, the Fermi motion of nucleons in nuclei could mask the effect.

(ii) A second interpretation involves the excitation of a giant dipole resonance that could be a source of the cusp phenomenon [13]). It has been shown that the cusp effects can be visible in the energy dependence of the pion induced reaction. The absorption channel has the advantage with respect to the elastic scattering channel for the observation the cusp phenomenon. A strong coupling of the inelastic channel with the pion absorption channel is due to the $1/v$ law behavior of the absorption cross section near the threshold.

(iii) On the other hand, still another interpretation would discuss this effect as a manifestation of the pionic degrees of freedom in nuclei [14]) where the low energy pions form additional doorways with groups of nucleons. One might expect that the creation of such a state most probably will lead to fragment emission. In fact, in the pion absorption reaction the pion energy would be preferentially given to the subsystem of nucleons that, with the pion, formed the doorway. The effect could manifest itself more strongly for the light nuclear targets since the Fermi motion of nucleons in heavy nuclei could mask the doorway mechanism.

Evidently, these interpretations are interexcluding. It may be an accidental coincidence in structure position for deuterium and carbon targets. Moreover, the

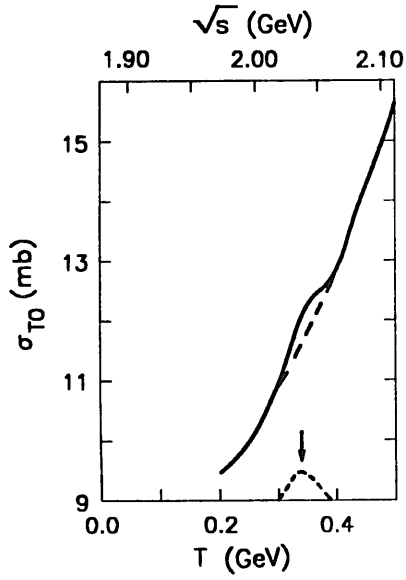

Fig. 9. $\sigma_{T0} = \sigma^{tot} + \frac{1}{2}\Delta\sigma_L - \Delta\sigma_T$ for pp interaction. Solid curve is a result of average of complete set of data for σ^{tot}, $\Delta\sigma_L$ and $\Delta\sigma_T$ [ref. [11])].

existence of the structure in the total cross section of the reaction $\pi^+ d \to pp$ needs confirmation.

5. Conclusion

New data on the total cross section of pion absorption on carbon with two protons in final state at pion kinetic energies 26–39 MeV is presented. Results show a dip less than 3 MeV of width (12%) in the cross section near a bombarding energy of 28.5 MeV.

Analysis of a second experiment focusing on $\pi^+ d \to pp$ at the same energies are underway and it is hoped that the results concerning elementary pion absorption will be very useful to clarify the situation.

We acknowledge valuable discussion on the problem considered with E.L. Mathie and E.W. Vogt. IIS wants to acknowledge the hospitality that TRIUMF extended to him.

References

1) D. Ashery and J.P. Schiffer, Ann. Rev. Nucl. Sci. **36** (1986) 207
2) I.I. Strakovsky, Czech, J. Phys. **B39** (1989) 843
3) I. Navon, D. Ashery, J. Alster, G. Azuelos, B.M. Barnett, W. Gyles, R.R. Johnson, D.R. Gill and T.G. Masterson, Phys. Rev. **C28** (1983) 2548;
K. Nakai, T. Kobayashi, T. Numao, T.A. Shidata, J. Chiba and K. Masutani, Phys. Rev. Lett. **44** (1980) 1446
4) R.L. Burman and M.E. Nordberg Jr, Phys. Rev. Lett. **21** (1968) 229;
W.R. Warton, P.D. Barnes, B. Bassalleck, R.A. Einstein, G. Franklin, R. Grace, C. Maner, P. Pile, R. Rieder, J. Szimanski, J.R. Comfort, F. Takeutchi, J.F. Amanu, S.A. Dytmann and K.G.R. Doss, Phys. Rev. **C31** (1985) 526
5) A.B. Laptev and I.I. Strakovsky, "Collection of experimental data for the reaction $pp \to \pi^+ d$". Petersburg, Nucl. Phys. Inst. Press vol. 1 (1985); vol. 2 (1986);
TRIUMF VAX System, 1990
6) B.G. Ritchie, Phys. Rev. **C28** (1983) 926
7) V.V. Abaev, E.P. Fedorova-Koval, A.B. Gridnerv, V.P. Koptev, S.P. Kruglov, Yu.A. Malov, G.V. Scherbakov, I.I. Strakovsky and N.A. Tarasov, J. of Phys. **G14** (1988) 903
8) Yu.K. Akimov, I.I. Haysak, D. Dorchioman, D. Lazarovich, S.I. Merzlyakov, K.O. Oganesyan, E.A. Pasyuk, S.Yu. Porokhovoy and A.I. Rudenko, Sov. J. PTE **4** (1981) 24
9) CERN Program Library, W505
10) J. Hoftiezer, Ch. Weddigen, P. Chatelain, B. Favier, F. Foroughi, C. Nussbaum, J. Piffaretti, S. Jaccard and P. Walden, Nucl. Phys. **A402** (1983) 429
11) A. Yokosawa, Int. J. Mod. Phys. **5** (1990) 3089
12) S.M. Bilenky and R.M. Ryndin, Phys. Lett. **6** (1963) 217;
P. Kroll, Phys. Data 22-1, Karlsruhe, 1981
13) M.Kh. Khankhasaev, JINR Preprint, E4-89-821, Dubna, 1989
14) G. Rowe and E.W. Vogt, Nucl. Phys. **A302** (1978) 511;
E.W. Vogt, private communication